AO26: Next-Generation Techniques for Monitoring Hazardous Weather from Space

Candidate number: 1005754
Supervisors: Dr. S. Proud and Prof. R. G. Grainger
Word count: 3933

Abstract

Above-anvil cirrus plumes, a cloud-top indicator of severe convective storms, are examined in a deep convective storm system in the Southeast US on May 18 2017, with the aim of estimating their height above the cloud anvil. Their signatures are observed using data from the GOES-16 Advanced Baseline Imager, and this data processed by the Optimal Retrieval of Aerosol and Cloud algorithm. When this processing did not accurately describe the properties of cirrus plumes, further methods were employed in an attempt to deduce the height of the above-anvil cirrus plumes. In the process, ECMWF temperature profiles were found to indicate that there might be a double tropopause in the region. An evaluation of the validity of the ECMWF profiles leads to uncertainty in whether they are an accurate representation of the atmosphere. As a result, no confident estimates for the heights of the plumes could be obtained from the data, with height estimates ranging from between 1 and 8 km above the anvil. These inconclusive results lead to discussion of whether passive sensing methods are suitable for such estimates.

1 Introduction

1.1 Satellite Observations of Severe Convective Storms

Severe convective storms can give rise to weather conditions such as hail and strong winds which can pose a risk to human life. Such storms also cause billions of dollars of property damage per year just in the United States [1]. As a result, the development of techniques for the short-term prediction of convective storms and their severity is of utmost importance.

The formation of severe storms is driven by convection. When the atmospheric temperature profile is such that there exists a high amount of available energy to induce convection (known as convective available potential energy, or CAPE), air parcels will move upwards and cool, allowing water vapour to condense out and form cloud droplets. Most convection will stop (unless air parcels have exceptionally high vertical momentum) when the atmosphere stops decreasing in temperature with height at the tropopause. Here, the updraft driving the cloud's formation will be redirected and the cloud droplets will spread horizontally, forming what is known as a storm 'anvil'.

Particularly severe storms tend to be associated with stronger updrafts, which can result in distinctive signature patterns on top of the anvil. For example, when an updraft is strong enough to lift some cloud material up beyond the tropopause into the lower stratosphere, a very cold region of cloud extending above the anvil is created, known as an overshooting top. When observed by satellites, these can be a very reliable indicator of severe weather being reported at the ground [2]. An overshooting top can sometimes interact with winds in the lower stratosphere, producing interesting textural features in the cloud top, such as above-anvil cirrus plumes.

1.2 Above-Anvil Cirrus Plumes

Above-anvil cirrus plumes (AACPs) are a cloud-top storm signature which seem to be associated with particularly severe storms [3]. They consist of 'plumes' of ice cloud which exist some distance above the top of the anvil of a convective storm, characterised by unique identifying patterns in visible and infrared satellite observations.

These were first observed as early as 1982, described by Fujita as 'jumping cirrus' in reference to their unusual height above the surrounding storm anvils [4], but in recent years, with the advancement of rapid-scan satellite observations, they have been subject to further study. AACPs have been observed to exist in the lower stratosphere, so their temperature appears warmer than the rest of the storm anvil, making them identifiable using infrared satellite imagery. Currently it is believed that the plumes are formed when overshooting tops interact with winds in the lower stratosphere resulting in either deformation of cloud material or gravity wave-breaking [5]. This produces the distinctive plume shape.

Attempts have been made to model the formation of these plumes [6, 7, 8] and to determine to what extent they are associated with severe weather [3]. There are still several open questions about AACPs. For example, the microphysics of the plumes is still uncertain, as well as how they can be used as a short-term predictor of severe weather, and why only some severe storms with overshooting tops will produce AACPs in a given region (or even within a given convective system).

An additional question is whether these plumes play a role in the injection of water into the lower stratosphere, which could have significant effects on stratospheric composition and chemistry [8]. It is hypothesised that convective storms transfer water from the troposphere to the stratosphere when strong updrafts create tropopause-penetrating overshooting tops [9, 10]. These updrafts have enough energy to overcome the cold trap at the tropopause, through which convection cannot usually continue to occur [11]. As a result, the lower stratosphere is one of the driest parts of the atmosphere. As water vapour is a powerful greenhouse gas, an increase in its stratospheric concentration results in a warming at the Earth's surface [12, 13]. For this reason, while AACPs are somewhat poorly understood, they could have significant impacts on climate change as well as on severe weather prediction.

1.3 Height of Above-Anvil Cirrus Plumes

The aim of this project was to use satellite data to investigate the height of AACPs above the storm anvil. Improved knowledge of exactly where AACPs exist would be useful for validating the mechanism for their formation, and hence furthering understanding of this process as a mechanism for stratospheric water injection. Current estimates of AACP height range between 1 and 6 km [5, 14, 15], partly deduced from modelling and partly from observations. As well as this, it could potentially be worth investigating whether a correlation between AACP height and storm severity exists, which could be useful in short-term storm forecasting.

2 Method

2.1 Data

2.1.1 Case Selection

The case examined during this project was a severe weather event in the Southeast US on May 18, 2017. On this date, a system of convective storms passed over this area, providing an excellent test bed for examining a series of AACPs. In particular, the storms present at 2330 UTC were examined. This case was selected as the SE US region is known for the frequency of severe convective storm systems [16], and because there were a number of AACP-producing storms present, which had already been analysed and located by Bedka [3].

2.1.2 Satellite Imagery

Data from the National Oceanic and Atmospheric Administration (NOAA) Geostationary

Orbiting Environmental Satellite (GOES) was used to examine the cirrus plumes. Observations of storms were based on mesoscale super-rapid-scan data from both visible and infrared imagery taken from the Advanced Baseline Imager (ABI) on GOES-16. The ABI has 16 channels of various wavelengths with a maximum spatial resolution of 0.5 km [17].

The mesoscale mode of the ABI instrument produces a 1000 by 1000 km image every 30 seconds. This 'super-rapid-scan' mode is very useful for tracking the evolution of convective storms. By observing successive images it is possible to deduce the horizontal wind direction and to confirm which AACPs are associated with which updrafts. Modelled datasets for atmospheric wind vectors are available, but in convection-dominated systems, these can be somewhat inaccurate as strong updrafts interfere with predicted macroscale wind directions. As a result, it is better to use the satellite data to deduce the wind speed and direction, especially in the lower stratosphere where convection will significantly affect anvil and AACP motion. Therefore, the rapid-scan satellite data was used to create an animation of the storms moving across the focus area to give a more reliable estimate of wind direction, providing some validation of the plume locations relative to the updrafts.

2.1.3 Temperature Profile Data

Cloud-top height can be determined from a measurement of cloud-top temperature and the local temperature profile. As a starting point, the atmospheric temperature profile was taken from the atmospheric high-resolution (HRES) 10-day operational dataset from the European Centre for Medium-range Weather Forecasting (ECMWF). This project used the direct model output of temperature against pressure and height levels. The data are provided in the form of 137 temperature measurements at various pressures, on a 0.5° by 0.5° latitude-longitude grid, recorded every six hours [18]. The temperature profiles are produced through a combination of modelling, prior information about the Earth system, and observations. Although this is the highest-resolution ECMWF product available, an average profile is not necessarily a good representation of the actual atmospheric temperature profile at convective scales.

To verify that the ECMWF profiles were reliable, they were compared to data from an atmospheric sounding at Fort Worth-Dallas (FWD), Texas. Here, a radiosonde in a weather balloon measures pressure, temperature, humidity, and wind speed as it ascends, giving us in-situ temperature profile measurements. The data used was provided by the Department of Atmospheric Science at the University of Wyoming [19].

2.2 Plume Identification

In order to analyse the AACPs, they were located using a combination of the satellite data and a database of storms provided by Bedka, used in his 2018 paper [3]. The raw data files from GOES were processed and visualised using PyTroll [20] in order to create images that could be used to manually identify and investigate the plumes. The database was used to plot individual storms with and without plumes on the satellite images.

2.3 Plume Height Estimation

2.3.1 ORAC

The first estimation of AACP heights was obtained using the Optimal Retrieval of Aerosol and Cloud (ORAC) algorithm, an optimal estimation scheme that determines a range of aerosol and cloud properties and their associated uncertainties using multispectral imagery [21]. Inputting the satellite data on a particular day allows ORAC to produce an estimate for the cloud-top temperature and hence cloud-top height, as well as various other quantities as a 500 by 500 grid of pixels across the study area. The ORAC process used in this case was a single-layer retrieval, meaning that the output only gives a single cloud-top temperature and height for each grid point.

The ORAC output was linearly interpolated across the grid to give a higher resolution of height estimates, allowing specific locations to be

probed more precisely, such as at the exact locations of cirrus plumes and overshooting tops. It should be noted that for the associated uncertainty outputs, the same method could not be used, so all uncertainty measurements are taken from the original ORAC output grid points.

2.3.2 Estimation via Temperature Profile

Improving the estimates of AACP heights beyond the ORAC output involved comparing the cloud-top temperature output from ORAC to the ECMWF temperature profiles. The various locations of a particular temperature's intersection with the profile allowed for further estimates of the possible vertical position of the top of the plume. Taken together with the constraint that AACPs must be above the anvil and hence the tropopause, their location should be possible to deduce given a standard atmospheric profile.

To apply this constraint, the tropopause height was calculated using the World Meteorological Organization's definition. This defines the tropopause as "the lowest level at which the lapse rate decreases to $2\,^{\circ}\mathrm{C\,km^{-1}}$ or less, provided that the average lapse rate between this level and all higher levels within 2 km does not exceed $2\,^{\circ}\mathrm{C\,km^{-1}}$." [22] The lapse rate Γ describes the rate at which atmospheric temperature T changes with altitude z, conventionally defined as

$$\Gamma = -\frac{\mathrm{d}T}{\mathrm{d}z}$$

3 Plume Identification

Shown in figure 1 are the locations of updrafts of individual convective storms across the study area in the Southeast USA. The storms and their associated AACPs were identified by an algorithm as described by Bedka [3].

Subfigure (a) shows a true-colour composite image, composed of visible and near-infrared wavelength bands that display the scene as it would be visible to the human eye. In this, updrafts with currently active AACPs are indicated by red squares, and those which are not currently producing AACPs are indicated by black squares. The plumes are most easily identifiable by their distinctive texture, appearing as smooth areas over the more complex texture of the top of the anvil, and the fact that they cast slight shadows on the anvil below.

The second image is a false-colour composite created using the visible $0.64\,\mu$m band (inverted, in red) and the $6.2\,\mu$m band (in green and blue). Here, the coldest parts of the cloud appear bright red. These very cold areas are usually the overshooting tops, which tend to occur at the indicated updrafts. The cirrus plumes can be identified as the warmer areas of the image in cyan. The storms currently producing AACPs are indicated in yellow, and those which are not in white. Note that some remnants of plumes still exist near storms which are identified as not currently producing AACPs; these plumes have drifted downwind and are no longer being actively produced.

4 ORAC Output

The ORAC output gives us two crucial datasets for this project. Firstly, it provides an estimate of cloud-top temperature, calculated using a combination of brightness temperatures from various ABI channels. Secondly, it provides an estimate of cloud-top height based on the estimated temperature and pre-processed temperature profiles (taken from the ECMWF data described in section 2.1.3). It also provides associated uncertainties for both of these.

Overall, the algorithm identifies the cloud-covered area of the convective system well, and does capture at least some of the vertical structure across the system. In particular, it appears to successfully estimate the heights of overshooting tops, suggesting that they extend a few kilometres above the tropopause as expected.

However, ORAC does not succeed at estimating the heights of AACPs. Where AACPs are identifiable in satellite images, ORAC interprets areas as being lower in height than the surrounding anvil. This implies either that the plumes

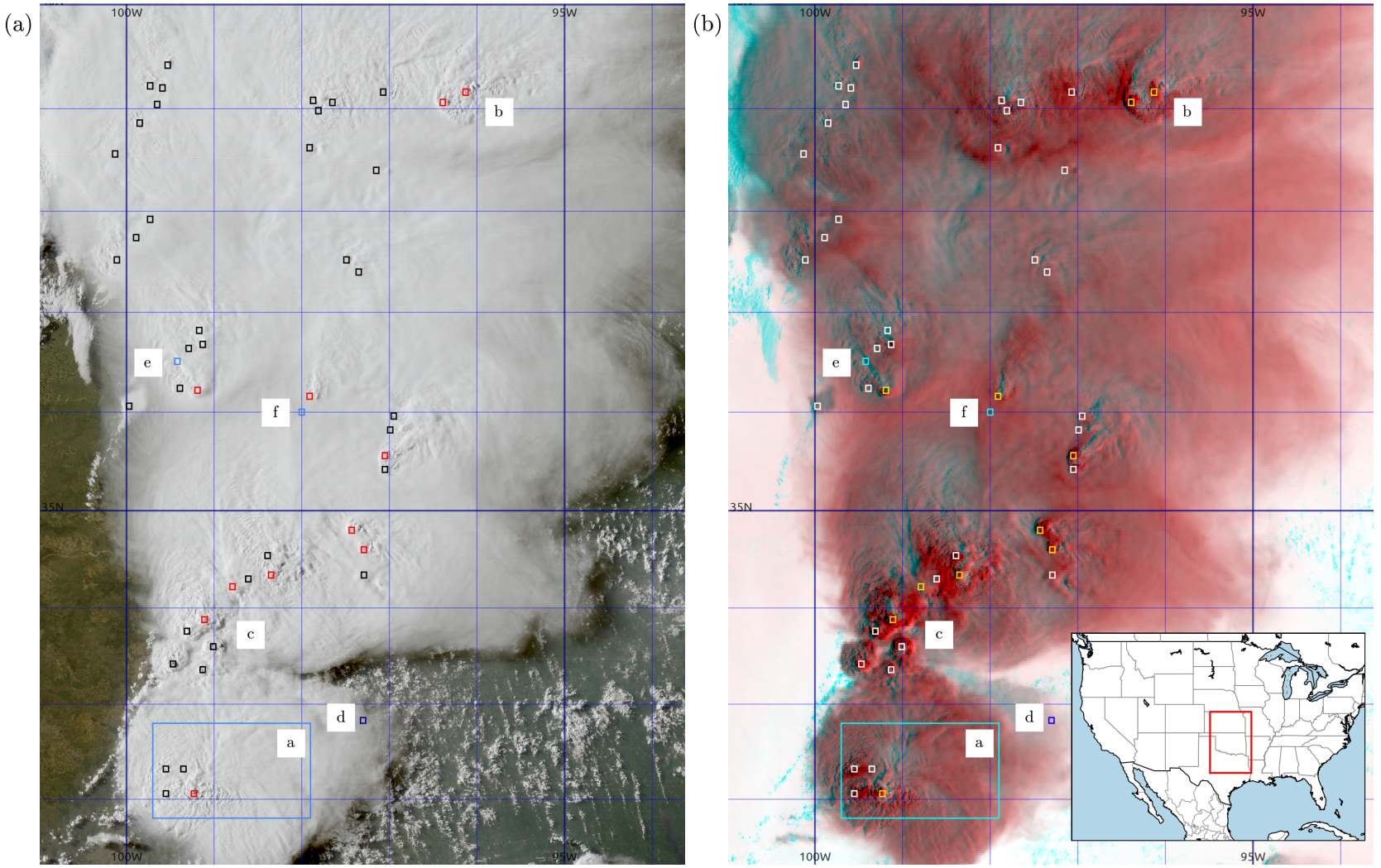

Figure 1: RGB composite images of the study area over the Southeast US. Images were created using the PyTroll Python package [20] to display data from GOES ABI channels at 2330 UTC on May 18, 2017. Relevant points referenced throughout the report are indicated with blue markers and labelled with letters. The inset map shows the location of the study area relative to North America.
(a) The true-colour composite, composed of visible channels centred on wavelengths of 0.64 μm and 0.47 μm as the red and blue colours, and an infrared channel 0.86 μm to act as a substitute green colour. Storms with active AACPs are indicated by red squares and storms without are indicated by black squares.
(b) A false-colour composite composed of the visible 0.64 μm band (inverted, in red) and the infrared 6.2 μm band (in green and blue). Storms with active AACPs are indicated by yellow squares and storms without are indicated by white squares.

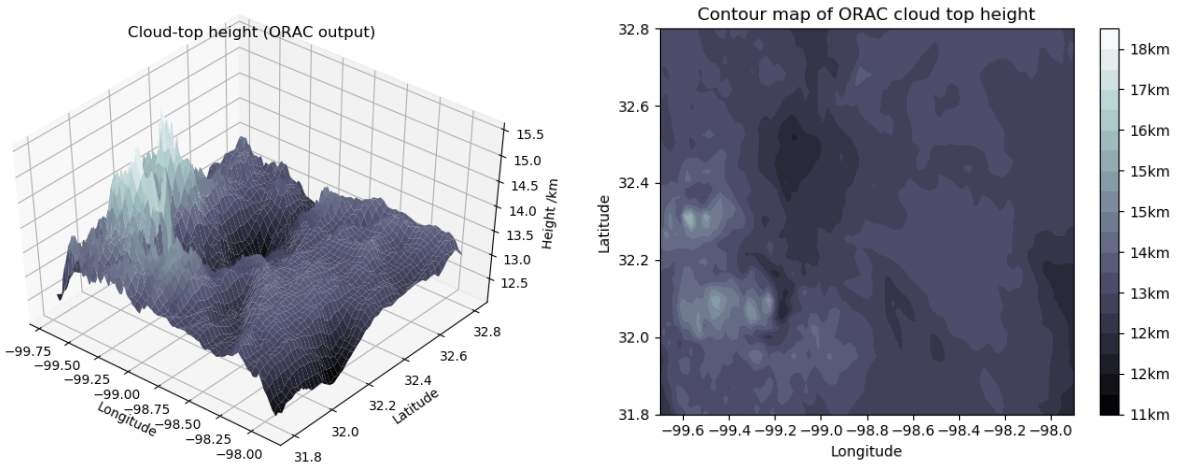

Figure 2: Cloud-top height as estimated by ORAC between 99.7° W, 31.8° N and 97.9° W, 32.8° N. This is indicated by the area illustrated as a blue rectangle labelled by box 'a' in figure 1. Clearly, the algorithm captures the overshooting tops that are seen in the SW corner of this section of the cloud, indicated by the lightest areas which reach heights of around 18 km, but places the height of the associated AACP (visible in the satellite imagery) as lower than the rest of the anvil.

were inside the anvil, or that these are areas of cloud where the anvil is around a kilometre lower than its usual height. The former is impossible, and the latter is clearly not the case as AACPs can be seen in figure 1, so it is reasonably certain that these heights are incorrect.

This is what one might expect from a single-layer retrieval, and does help to identify the locations of the cirrus plumes even if ORAC's ability to determine their height is limited. The height output is also useful in the later stages as an approximation for anvil height, as are the cloud-top temperatures which allow further AACP height estimates to be made.

4.1 Uncertainties

The associated uncertainties for both the cloud-top height and temperature provide further insight into the reliability of this output. For both height and temperature, there are relatively high uncertainties over the anvil. Height has uncertainties of up to 5 km consistently for large areas of the cloud, and temperature has uncertainties which are consistently above 12 K across the anvil. These are even higher in areas where plumes are observed, which suggests that even though the ORAC heights are incorrect, the algorithm is nonetheless correctly identifying that this data is uncertain and of low quality.

5 The Double Tropopause

The next stage of improving the estimates was using the ECMWF temperature profiles to calculate alternative heights for the AACPs. For a typical temperature profile, this would result in one other possible height for the plume in the lower stratosphere, giving a sensible estimate for the location of the plumes where the cloud-top is warmer. However, the atmospheric temperature profiles of the region are far from standard. Two examples of these are shown in figure 3.

Over most of the area investigated, the ECMWF temperature profiles exhibit some complex behaviour at altitudes between 12 and 20 km. Throughout the cloud-covered areas there appears to be a double tropopause. That is, after the temperature begins to increase above the lowest temperature inversion, the lapse rate reverses and atmosphere begins to cool again until it reaches a second temperature inversion, after which it continues to increase normally through the stratosphere.

Multiple tropopauses are not unheard of [23].

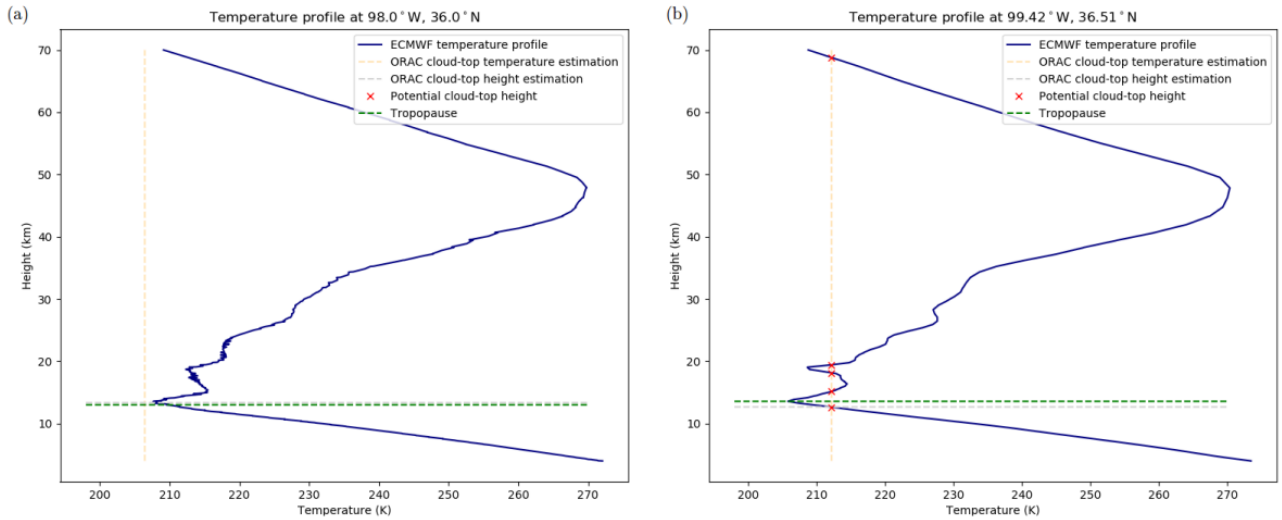

Figure 3: Temperature profiles and the associated ORAC cloud-top temperature and height outputs at two representative locations in the study area.
(a) Temperature profile of a normal area of the anvil, marked as box 'e' in figure 1. ORAC has extrapolated the tropopause temperature profile to find an estimated anvil height associated with this temperature, which is colder than any of the temperatures that the ECMWF profile predicts.
(b) Temperature profile of a cirrus plume, marked as box 'f' in figure 1. Here, there are four heights where the AACP could be, including three above the tropopause, if you find the intersections of the cloud-top temperature and profile (ignoring the point in the high thermosphere).

The World Meteorological Organization defines a second tropopause as any place where the tropopause condition is met again, if the average lapse rate in the kilometre above the first tropopause exceeds $3\,^{\circ}\mathrm{C\,km^{-1}}$ [22]. In fact, double tropopauses can even be relatively common in certain areas, including the Southeast US [24].

Whether the ECMWF profiles genuinely reflect the atmospheric profile at this time is uncertain for several reasons. Firstly, the ECMWF profiles are relatively low-resolution, both temporally and in terms of the latitude and longitude coordinates, so interpolated profiles between these points may not be accurate. Secondly, they are largely modelled data based on combinations of measurements above and below the cloud [18]. Where there is thick cumulonimbus cloud, as is the case here, the temperature profiles may become unreliable around the height of the cloud if there are inconsistencies between the data from above and below the cloud layer. This would be consistent with the unusual signal in the data around the expected tropopause height at this latitude, especially in areas where the anvil is present.

However, it is not possible to rule out the existence of a double tropopause in this region. They have been observed to exist here semi-frequently, and in the satellite composites, the areas near the labels 'b' and 'c' in figure 1 could potentially be mini-anvils which exist at the second tropopause rather than the first. This would likely not be identified in the ORAC output due to the way in which ORAC calculates cloud-top height.

To check the validity of the ECMWF profiles, they were compared to data from an atmospheric sounding (provided by the University of Wyoming). The only station within the study area which was near any cloud at the time of the reading was the FWD station at 93.30° W, 32.83° N, labelled in figure 1 as the dark blue marker by box 'd'. Unfortunately at the nearest reading time to the storm event, the area was still not fully covered by cloud and the associated ECMWF profile at this location did not exhibit the characteristic double tropopause which

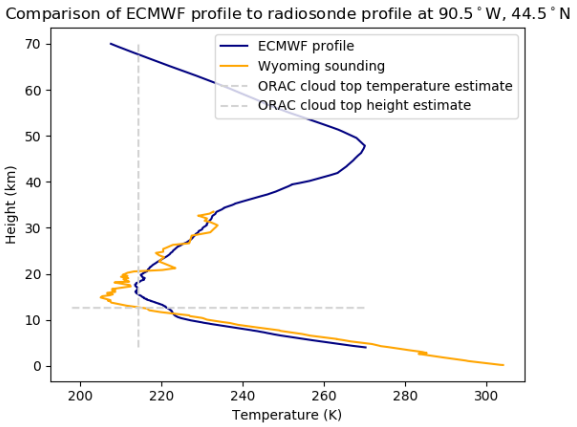

Figure 4: A comparison of the measured radiosonde atmospheric profile (data provided by the University of Wyoming), with the ECMWF profile at this point. Here, the double tropopause is less obvious than in figure 3, and there does not appear to be very significant deviation in the shape of the ECMWF profile from the observed sounding.

appears through much of the anvil.

The comparison of the atmospheric sounding data and ECMWF profile at the sounding location is shown in figure 4. While the atmospheric sounding did not directly contradict the data, it is not within the main body of the anvil. Therefore, it is still inconclusive as to whether the double tropopause genuinely does exist over the anvil, or whether it is simply an anomaly arising from the method of generating ECMWF profiles. It should be noted that if the double tropopause does exist in the area, it could have interesting impacts on the effects of water transport into the stratosphere as discussed in section 1.2, and examined by Homeyer in 2014 [25].

6 Alternative AACP Height Estimates

Regardless of whether the double tropopause exists, the profiles fluctuate significantly anyway, to the extent that in many locations there are a number of points where the cloud-top temperature intersects with the atmospheric profile above the tropopause. This gives a wide range of possible plume heights, ranging from between around 2 km to around 8 km above the tropopause, as illustrated in figure 3b. This is a significant range, not even improving on the uncertainty of ORAC's height estimates.

It is possible to derive some estimate of cloud-top height from these possible heights, however. The most logical first estimate of where the plumes exist is obtained by selecting as low a height as possible above the first tropopause. Using the rest of the anvil's temperature as a baseline, it was possible to identify AACP locations and remap their ORAC output heights to more realistic heights in the lower stratosphere (or inter-tropopause layer, as the case may be). However, this did involve making the assumption that the actual height of the plume lies on the first 'branch' of the temperature profile above the (first) tropopause.

Calculating these heights over areas with plumes gives results as demonstrated in figure 5, which shows the estimates of cloud-top height in the area from 99.7° W to 97.9° W and 31.8° N to 32.8° N. The blue gradient dots represent the remapped heights above the anvil, while the greyscale surface plot represents the ORAC cloud-top height estimates in this area.

The location of the AACPs visible here is consistent with what one might expect. By comparing this with the wind direction, images, and storm database, it is reasonably confident that the actual location of plumes matches up well with where the algorithm changes the heights of the ORAC output.

Furthermore, this remapping estimates cirrus plumes as around 3-5 km above the top of the rest of the anvil. This is at a few kilometres above the associated overshooting top, but AACPs have previously been observed to be up to 5 km above the tropopause [14], so this is not unexpected. However, in other areas, the same algorithm remaps the points to give height estimates of around 1-3 km above the anvil. This indicates that there is a wide variety of possible heights for the plumes depending on the properties of the associated updrafts and surrounding cloud.

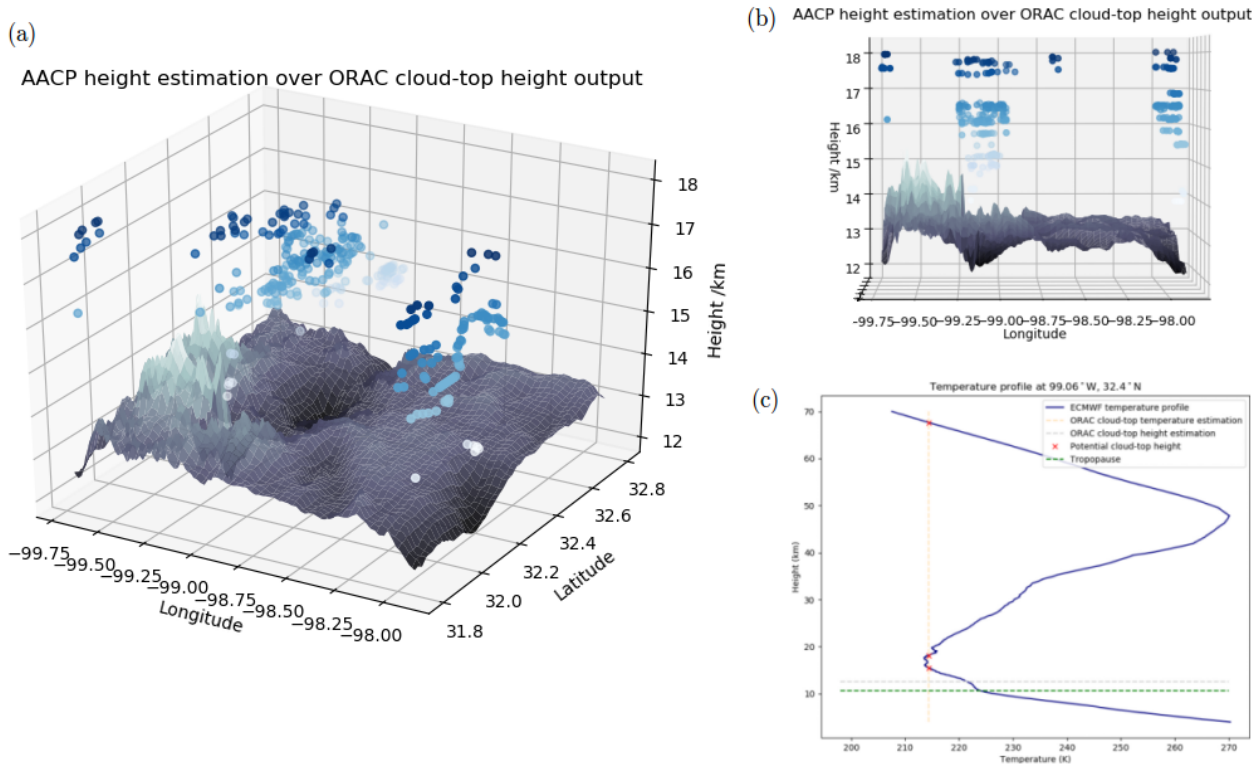

Figure 5: An illustration of the remapped heights of the cirrus plumes above the storm anvil.
(a) The greyscale surface plot represents the ORAC height output (the same as that illustrated in figure 2) in the focus area indicated by box 'a' in figure 1. The blue dots are the points which have been remapped, and become darker blue as altitude increases. The plumes tend to exist over the lowest areas of ORAC height output, represented by the darkest grey sections of the surface.
(b) This angle gives a better indication of the heights of the remapped points, suggesting that the cirrus plumes exist at heights between 2 and 5 km above the anvil.
(c) A temperature profile of an example point in this grid at 99.06° W, 32.4° N. The remapped height estimate gives a height of around 18 km as opposed to around 14 km. Note that the tropopause definition here was inadequate and places it lower than one might intuitively place it. Interestingly, this area does not have as distinct a double tropopause as much of the rest of the anvil.

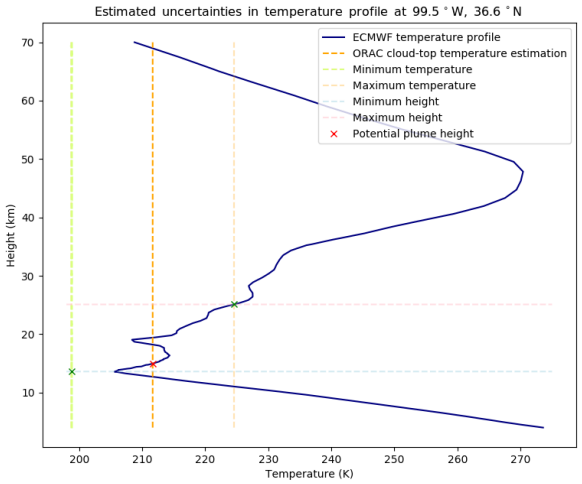

Figure 6: A temperature profile at an ORAC output point at around 99.5° W, 36.6° N. ORAC's cloud-top temperature uncertainty is used to determine an uncertainty for the AACP height estimate. This is around 10 km. The minimum possible height is set at the tropopause, since the plume cannot exist lower than the top of the storm anvil.

6.1 Uncertainties

The numerical uncertainty in the AACP height was estimated by calculating the minimum and maximum possible heights that are associated with the minimum and maximum possible temperatures as indicated by the ORAC cloud-top temperature uncertainty. Due to the very large uncertainties in cloud-top temperature, there is a correspondingly huge uncertainty in height: the AACP could be anywhere within a 10 km range, as illustrated in figure 6. This renders the assumption of the height being on the first above-tropopause branch irrelevant, since the actual location of the plume could be at such a wide range of heights.

Furthermore, given our discussion in section 5, it is somewhat unlikely that the temperature profiles used to calculate AACP heights are accurate. This limits how reliable the estimates are, as they depend almost entirely on the temperature profiles being correct for each plume, but the resolution of the ECMWF profiles is inadequate for this purpose.

7 Conclusions

The large uncertainties in both the temperature profiles and the ORAC cloud-top temperature means that it is hard to draw concrete conclusions about AACP heights from this case study. However, the estimates are more accurate than those deduced from the single-layer ORAC retrieval (here used because a multi-layer retrieval of such a complex cloud-top structure would have been inaccurate and computationally intensive). Two-layer retrievals are most effective if an initial estimate of cloud-top heights can be given. Therefore, these height estimates could be useful as input parameters in a multi-layer retrieval.

Also, the project has proved to be a productive investigation into the limitations of ECMWF temperature profiles and ORAC output. Further work into understanding how ECMWF profiles are generated, and how this affects their output around convective systems, would have far-reaching impacts wherever these profiles are used. Any inconsistencies could be integrated into ORAC or other algorithms which use this dataset to better inform uncertainty output, or correct for systematic errors in the profiles.

Finally, the project has been fairly conclusive in one respect: passive sensing methods are generally not adequate for calculating the physical heights of complex cloud-top structures. The uncertainties are so significant that these results are extremely approximate. In order to examine the height and other properties of AACPs, further work should be carried out using active sensing methods. For example, LIDAR (a method of measuring distance using pulsed light and reflections) could be used to obtain a more reliable estimate of the height of the cirrus plumes, and in-situ aircraft measurements could be used to take better readings of their temperature.

While such methods would be much more limited in terms of data quantity, they would be much more reliable, and could be used to validate data from passive sensing methods. Until temperature profiles are more reliable and much higher in spatial resolution, active sensing methods are likely to be vastly more useful for making these kinds of measurements.

Acknowledgements

I would like to thank my supervisors, Dr Simon Proud and Prof Don Grainger, for their guidance, support, and patience throughout the project and subsequent write-up. As well as this, I've received invaluable feedback from the whole of the Earth Observation Data Group, and would especially like to thank Isabelle Taylor and Adam Povey for their kind support and advice. Finally, thanks to Mark and Lauren for proofreading.

References

[1] I. Loomis. Hail causes the most storm damage costs across north america. *EOS*, 99, August 2018.

[2] Kristopher M. Bedka, John T. Allen, Heinz Jurgen Punge, Michael Kunz, and Denis Simanovic. A long-term overshooting convective cloud-top detection database over australia derived from mtsat japanese advanced meteorological imager observations. *Journal of Applied Meteorology and Climatology*, 57(4):937–951, 2018.

[3] Kristopher Bedka, Elisa M. Murillo, Cameron R. Homeyer, Benjamin Scarino, and Haiden Mersiovsky. The above-anvil cirrus plume: An important severe weather indicator in visible and infrared satellite imagery. *Weather and Forecasting*, 33(5):1159–1181, 2018.

[4] T. Fujita. Principle of stereoscopic height computations and their applications to stratospheric cirrus over severe thunderstorms. *J. Meteorol. Soc. Jpn.*, 60, March 1982.

[5] Pao K. Wang. Moisture plumes above thunderstorm anvils and their contributions to cross-tropopause transport of water vapor in midlatitudes. *Journal of Geophysical Research: Atmospheres*, 108(D6), 2003.

[6] Pao K. Wang. A cloud model interpretation of jumping cirrus above storm top. *Geophysical Research Letters*, 31(18), 2004.

[7] Pao K. Wang. The thermodynamic structure atop a penetrating convective thunderstorm. *Atmospheric Research - ATMOS RES*, 83:254–262, February 2007.

[8] Pao Wang, Shih-Hao Su, Zdenk Charvt, Jindich stka, and Hsin-Mu Lin. Cross tropopause transport of water by mid-latitude deep convective storms: A review. *Terrestrial, Atmospheric and Oceanic Sciences*, 22:447, October 2011.

[9] Martin Setvák, Daniel Lindsey, Robert Rabin, Pao Wang, and Albeta Demeterov. Indication of water vapor transport into the lower stratosphere above midlatitude convective storms: Meteosat second generation satellite observations and radiative transfer model simulations. *Atmospheric Research*, 89:170–180, July 2008.

[10] Jessica B. Smith, David M. Wilmouth, Kristopher M. Bedka, Kenneth P. Bowman, Cameron R. Homeyer, John A. Dykema, Maryann R. Sargent, Corey E. Clapp, Stephen S. Leroy, David S. Sayres, Jonathan M. Dean-Day, T. Paul Bui, and James G. Anderson. A case study of convectively sourced water vapor observed in the overworld stratosphere over the united states. *Journal of Geophysical Research: Atmospheres*, 122(17):9529–9554, 2017.

[11] Gordon Miller Bourne Dobson, A. W. Brewer, and B. M. Cwilong. Bakerian lecture: Meteorology of the lower stratosphere. *Proceedings of the Royal Society of London. Series A. Mathematical and Physical Sciences*, 185(1001):144–175, 1946.

[12] Susan Solomon, Karen H. Rosenlof, Robert W. Portmann, John S. Daniel, Sean M. Davis, Todd J. Sanford, and Gian-Kasper Plattner. Contributions of stratospheric water vapor to decadal changes in the rate of global warming. *Science*, 327(5970):1219–1223, 2010.

[13] Yuan Wang, Hui Su, Jonathan H. Jiang, Nathaniel J. Livesey, Michelle L. Santee, Lucien Froidevaux, William G. Read, and John Anderson. The linkage between stratospheric water vapor and surface temperature in an observation-constrained coupled general circulation model. *Climate Dynamics*, 48(7):2671–2683, April 2017.

[14] Cameron R. Homeyer, Joel D. McAuliffe, and Kristopher M. Bedka. On the development of above-anvil cirrus plumes in extratropical convection. *Journal of the Atmospheric Sciences*, 74(5):1617–1633, 2017.

[15] Vincenzo Levizzani and Martin Setvák. Multispectral, high-resolution satellite observations of plumes on top of convective storms. *Journal of the Atmospheric Sciences*, 53(3):361–369, 1996.

[16] NOAA. Thunderstorm basics. Web page, accessed 4 April 2019.

https://www.nssl.noaa.gov/education/svrwx101/thunderstorms/.

[17] GOES-R Series Program Office. ABI bands quick information guides. Web page, February 2015, accessed 14 March 2019. https://www.goes-r.gov/education/ABI-bands-quick-info.html.

[18] R G Owens and T D Hewson. ECMWF forecast user guide. May 2018.

[19] University of Wyoming. Web page, accessed 3 March 2019. http://weather.uwyo.edu/upperair/sounding.html.

[20] Martin Raspaud, David Hoese, Panu Lahtinen, Adam Dybbroe, Lars rum Rasmussen, Stephan Finkensieper, William Roberts, sjoro, Thomas Leppelt, BENR0, Ulrik Egede, Mikhail Itkin, Eysteinn Sigursson, howff, Satellite Radar, Nowcasting Division, Trygve Aspenes, hazbottles, ColinDuff, Cody, lorenzo clementi, Marc Honnorat, roquetp, oananicola, praerien, Tom Parker, RutgerK, ralphk11, JohannesSMHI, Chris Lamb, and Antonio Valentino. pytroll/satpy: Version 0.12.0, February 2019.

[21] C. A. Poulsen, R. Siddans, G. E. Thomas, A. M. Sayer, R. G. Grainger, E. Campmany, S. M. Dean, C. Arnold, and P. D. Watts. Cloud retrievals from satellite data using optimal estimation: evaluation and application to atsr. *Atmospheric Measurement Techniques*, 5(8):1889–1910, 2012.

[22] World Meteorological Organization (WMO). Definition of tropopause and of significant levels. *WMO Bulletin*, 6(4):136–7, October 1957.

[23] Juan Antonio Añel, Laura de la Torre Ramos, and Luis Gimeno. On the origin of the air between multiple tropopauses at midlatitudes. *The Scientific World Journal*, 2012:191028, May 2012.

[24] Tanya R. Peevey, John C. Gille, Cora E. Randall, and Anne Kunz. Investigation of double tropopause spatial and temporal global variability utilizing high resolution dynamics limb sounder temperature observations. *Journal of Geophysical Research: Atmospheres*, 117(D1), 2012.

[25] Cameron R. Homeyer, Laura L. Pan, Samuel W. Dorsi, Linnea M. Avallone, Andrew J. Weinheimer, Anthony S. O'Brien, Joshua P. DiGangi, Mark A. Zondlo, Thomas B. Ryerson, Glenn S. Diskin, and Teresa L. Campos. Convective transport of water vapor into the lower stratosphere observed during double-tropopause events. *Journal of Geophysical Research: Atmospheres*, 119(18):10,941–10,958, 2014.